PROCEEDINGS OF SCIENCE

Long-term AGN variability and the case of GSN 069

Richard Saxton[*]
XMM-Newton SOC, ESAC, Apartado 78, E-28691 Villanueva de la Cañada, Madrid, Spain
E-mail: richard.saxton@sciops.esa.int

Andrew Read
Dept. of Physics and Astronomy, University of Leicester, Leicester LE1 7RH, U.K.
E-mail: amr30@star.le.ac.uk

Pilar Esquej
Centro de Astrobiología (CSIC-INTA), E-28850 Torrejon de Ardóz, Madrid, Spain
E-mail: pilar.esquej@cab.inta-csic.es

Giovanni Miniutti
Centro de Astrobiología (CSIC-INTA), ESAC, Apartado 78, E-28691 Villanueva de la Cañada, Madrid, Spain
E-mail: gminiutti@cab.inta-csic.es

Emilio Alvarez[†]
ESAC, Apartado 78, E-28691 Villanueva de la Cañada, Madrid, Spain
E-mail: ealvarez@gae.ucm.es

We report on a study of long-term flux variations in a sample of more than 1000 AGN observed with ROSAT and in the XMM-Newton slew survey. Over a period of 3-19 years, NLS1 galaxies as a class are found to be only slightly more variable than broad line Seyfert galaxies, despite the strong short term variability seen in some bright nearby NLS1s. Contrary to expectations, it is Seyfert II galaxies that exhibit the greatest flux volatility. One particular Sy II, which has brightened by a factor > 300 over 15 years, has been monitored in detail with Swift and XMM. The spectrum is extremely soft (kT $\sim$ 60eV) consistent with pure thermal emission from an accretion disk and reminiscent of ROSAT observations of the NLS1, WPVS 007. We show that this is likely to be a "true" Sy II, without a BLR, and speculate that in its new high luminosity state we may be able to witness a BLR in formation.

Narrow-Line Seyfert 1 Galaxies and their place in the Universe - NLS1,
April 04-06, 2011
Milan Italy

[*]Speaker.
[†]Current address: Universidad Complutense, E-28040 Madrid, Spain

PoS(NLS1)008

1. Introduction

The variability of the radiation output of AGN is well established and is one of their defining characteristics. In single observations of Seyfert I galaxies, fluctuations in the X-ray output on timescales of minutes to hours is the norm (e.g. NGC 4051 [1] and MRK 766 [2]). The power spectral density function (PSD) of these variations can be described by red noise; a smooth spectrum with increasing amplitude at lower frequencies ([3]) . The PSD of AGN has been shown to have a break, where the slope flattens, occurring on a timescale that scales with the luminosity and by implication the black hole mass. Lower mass (luminosity) AGN have a break in the PSD of $\sim 10^{-2}$ days (e.g. NGC 4051 [4]) whereas the most massive AGN have breaks at ~ 100 days (e.g. NGC 3516 [5]). This means that on short timescales, low mass AGN exhibit stronger X-ray variability than their more massive counterparts whereas on timescales of years the variability should be consistent. An additional dependence on the fraction of the Eddington accretion rate, $\dot{m}$ has been observed, leading to the refinement that the variability can be explained by characteristic pertubations in a steady-state accretion disk, whose inner radius scales with $M_{BH}/\dot{m}$ [6].

The class of objects known as NLS1, show stronger variability than Sy I and exhibit more rapid variations. This is consistent with the belief that they are low mass systems accreting at a high fraction of the Eddington rate.

Very large changes in flux due to variations in line-of-sight absorbing material have been observed in several sources. In the Seyfert 1.8 galaxy, NGC1365, factor 10 variations, accompanied by strong spectral changes have been seen several times ([7], [8]) and can be modelled by movements of individual clouds in the broad-line region.

Finally, Bl Lacs or Blazars have been famous for their volatility at all wavelengths for a long time (e.g. [9]).

While there has been a lot of work on short-timescale variations in specific sources and longer baseline studies of bright sources with RXTE, to date there have been few systematic studies of the variability of large samples of objects. This is mainly due to the lack of large-area sensitive sky surveys. The ROSAT All Sky Survey (RASS [10]) is an excellent resource for AGN with $F_{0.2-2} > 3 \times 10^{-13}$ erg s^{-1} cm^{-2} but it can only be systematically compared with data taken from ROSAT pointed observations taken months or a few years after the RASS completed in 1990. With the advent of the XMM-Newton slew survey (XMMSL1 [11]) containing observations from 40% of the sky with $F_{0.2-2} > 6 \times 10^{-13}$ erg s^{-1} cm^{-2}, a sensible comparison of AGN flux over a baseline of 3-19 years can now be achieved over 40% of the sky. In this paper we make a systematic comparison of the long-term variability of all classes of AGN detected either in the ROSAT or XMMSL1 surveys. A λCDM cosmology with $(\omega_M, \omega_\lambda)$ = (0.3,0.7) and H_0=70 km^{-1}sec^{-1} Mpc^{-1} has been assumed throughout.

2. Method of ROSAT/XMM comparison

We have made a sample of AGN which have been observed (but not necessarily detected) in both the RASS, or ROSAT pointed observations, and XMMSL1. We define three groups of objects:

- XMMSL1 sources, identified as AGN or galaxies, which have counterparts in ROSAT.

- XMMSL1 sources, identified as AGN or galaxies, which have been observed but not detected by ROSAT.

- RASS sources, identified as AGN or galaxies, which have been observed but not detected in XMMSL1.

We have used sources from the XMMSL1-delta3 CLEAN catalogue, released in August 2009, containing slew data taken between August 2001 and January 2009.

Sources which are detected with extended X-ray emission in either XMM-Newton or ROSAT have been excluded.

2.1 Upper limits

For the XMMSL1 AGN without a ROSAT counterpart a 2-sigma upper limit to the ROSAT count rate has been found using the EXSAS software package ([12]).

For RASS AGN, observed but not detected in XMMSL1, we have calculated a 2-sigma upper limit to the XMM-Newton count rate using a web-based upper limit server[1] ([13]).

The final sample contains 1038 AGN of which 689 were detected in both surveys, 223 have a RASS upper limit and 126 have an XMMSL1 upper limit.

2.2 Count rate to flux conversion

All XMM-Newton slew observations have been made with the EPIC-pn detector using the Medium filter. In Figure 1 we plot the XMMSL1, 0.2–2 keV count rate against the RASS count rates. We find the mean ratio of the XMM to RASS count rates is 6.94+/-0.20. From now on we use a factor 7 to normalise the count rate ratio, such that an intrinsic ratio of 7 is considered to show the same 0.2-2 keV flux in the two missions. The conversion factor from count rate to flux is crucial for comparing fluxes from different instruments and we need to be very careful when considering the effect of the source spectrum on this conversion. In Figure 2 we show the count rate ratio (normalised by the factor 7; R_7) as a function of the source spectrum. In principle there is a large variation of R_7 if the absorbing column is very low or very high. With these AGN observations, NH is practically limited to a minimum of $\sim 1 \times 10^{20}$ cm^{-2}, due to our Galaxy, and a maximum of $\sim 10^{22}$ cm^{-2} due to the flux limitations of the two surveys[2]. This can be seen clearly in the sky distribution of the objects in the sample where few objects lie in the Galactic plane (Fig. 3). Similarly we can infer that the intrinsic absorption can not much exceed $\sim 10^{22}$cm^{-2}. In this range, and for spectral slopes of 1.0 to 3.0, we see that a source with equal flux in RASS and XMMSL1 observations will have $0.3 < R_7 < 1.5$.

We now define the variability ratio, R_V, to be the ratio between the higher and lower count rate irrespective of the observatory[3]

[1] http://xmm.esac.esa.int/external/xmm_products/slew_survey/upper_limit/uls.shtml

[2] This applies to cold absorption. The behaviour of ionized absorbers which permit the passage of low-energy X-rays is quite different

[3] Hence $R_V = 1$ when $R_7 = 1$ and $R_V = 2$ when $R_7 = 2$ or $R_7 = 0.5$.

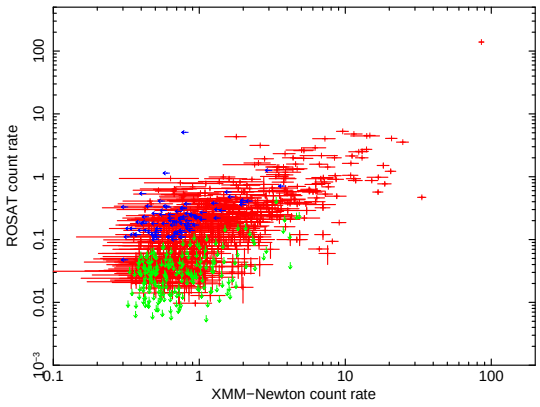

Figure 1: A comparison of the ROSAT and XMM-Newton (0.2–2 keV) slew count rates

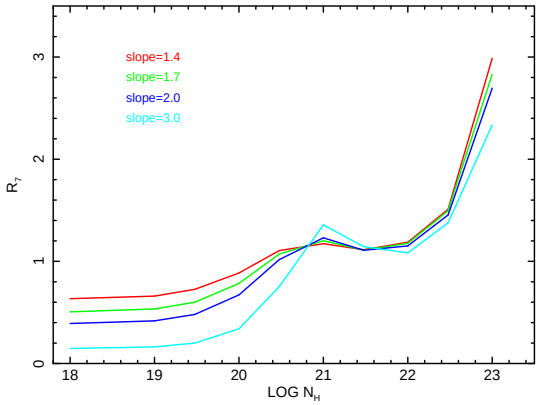

Figure 2: The influence of source spectra (an absorbed power-law) on the XMMSL1 / ROSAT count rate ratio

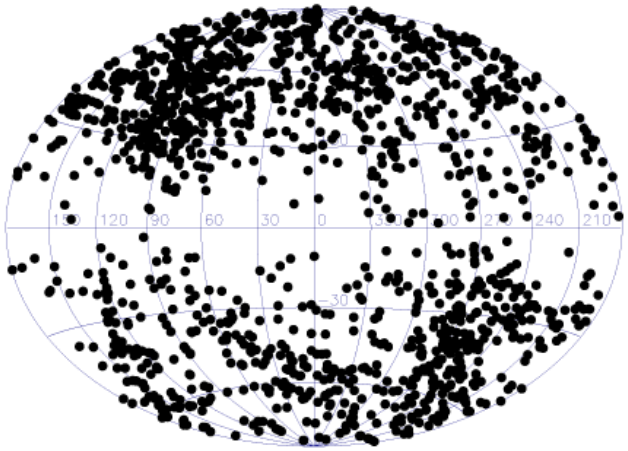

Figure 3: The sky distribution of the AGN in the sample in Galactic coordinates

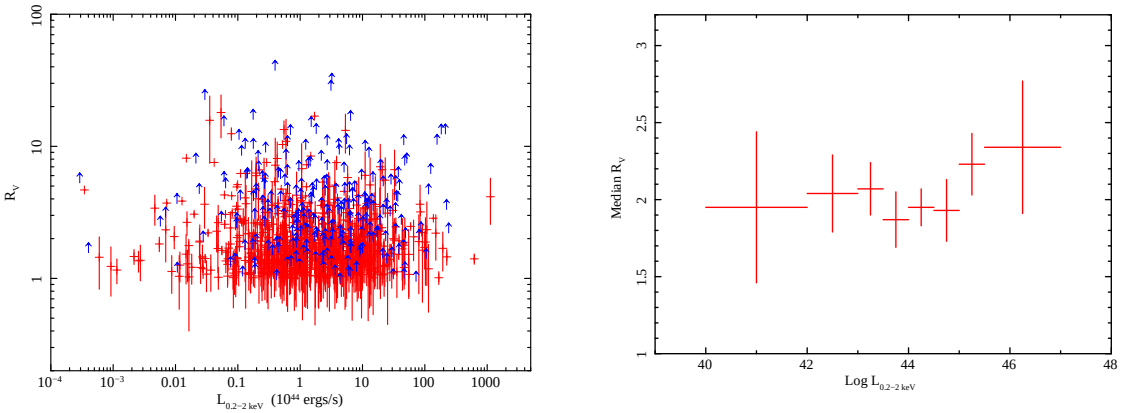

Figure 4: The X-ray variability of our sample as a function of XMMSL1 0.2–2 keV luminosity; left panel: individual sources, right panel: median variability per luminosity bin.

3. Results of ROSAT/XMM comparison

From the full population of 1038 AGN we find a median count rate ratio ($\hat{R_V}$) of 2.11, with 68.4% of the sources having $R_V \leq 3$ and 4.9% with $R_V \geq 10$.

We have made simulations of a non-varying population of sources with the Galactic N_H randomly selected from the actual sky values of the 1038 AGN, power-law indices selected from the population of ROSAT AGN slopes reported in [14] ($\Gamma = 2.05 \pm 0.55$) and count rates randomised using the actual errors in the XMMSL1 and RASS measurements. The simulated sources have a variability ratio with a median value $\hat{S_V}$=1.295 $\pm$ 0.003.

Following, [16] and [17] we calculate the true variability signal (V) by:

$$V^2 = (R_V - 1)^2 - (S_V - 1)^2 \tag{3.1}$$

where S_V is effectively the noise due to the spectral effects and measurement errors. This gives a median variability, V, of 107 $\pm$ 7% in the 0.2–2 keV energy band. In the UV band the mean long-term variability was found to be 35% from a survey of 9000 SDSS quasars ([18]). This result then continues the trend of higher photon frequencies exhibiting larger amplitude variability, seen on shorter timescales (e.g. NGC 5548; [19]).

3.1 Luminosity dependence

In Fig. 4 we plot R_V against the X-ray luminosity for the sources where the redshift is known. No significant correlation is found. As we are probing variability timescales far longer than the PSD break timescale it is normal that the luminosity-dependence, seen at shorter timescale, has no influence. This result shows that no further luminosity (mass) dependent effect is affecting the longer-term variability.

3.2 Source category

We have cross-correlated our sample with the Veron catalog of Quasars & AGN [22] to find the AGN class for each source, where known. In Table 1 we separate the sources by AGN class and

Table 1: Variability statistics for each AGN class

CLASS[a]	No.[b]	Median[c]	Fraction (%)[d]		
		Var. (%)	$R_V < 2$	$R_V < 3$	$R_V > 10$
ALL	1038	107 ± 7	46.8	68.4	4.9 ± 0.8
S1	318	90 ± 12	51.8	72.0	4.1 ± 1.4
S1.2	48	66 ± 27	62.5	78.9	0.0
S1.5	83	112 ± 26	45.1	65.7	3.3 ± 2.4
S1.8/1.9/2	37	155 ± 44	34.3	55.9	13.3 ± 6.0
QSO	232	130 ± 18	42.4	62.1	4.8 ± 2.0
NLS1	64	99 ± 28	48.1	72.5	4.1 ± 2.9
Blazar	142	109 ± 19	43.9	73.4	3.4 ± 1.7

[a] AGN class: Seyfert 1, 1.2, 1.5, a combination of 1.8, 1.9 and 2, QSO, NLS1 and a combination of Blazars, blazar candidates and highly polarised quasars.
[b] The total number of sources in this category.
[c] Median variability, $\hat{V}$, expressed as a percentage, after correcting for spectral effects (see text).
[d] The percentage of sources with R_V less than 2, less than 3 or greater than 10.

calculate the median variability and the fraction of sources showing $R_V < 2$, < 3 and > 10. The calculations ignore sources with upper limits that fall outside of these limits.

Seyfert II galaxies have the highest percentage of sources showing strong ($R_V > 10$) variability. It is not clear whether this is due to changes in line-of-sight absorption or changes in the intrinsic emission and these data can not help distinguish between the two possibilities. A closer look at one particular example is needed.

4. GSN 069

During a slew on July 14, 2010 XMM-Newton detected soft X-ray emission at 1.5 ± 0.3 counts s^{-1} from a position consistent with the nucleus of GSN 069 (also known as 6dFg0119087-341131; z=0.01816) (see Fig. 5). Previous ROSAT survey and pointed observations failed to detect the source and give upper limits, to the unabsorbed flux, 30–360 times fainter than the XMM-Newton slew detection (Table 2).

Two, consistent, optical spectra, taken in 2001 and 2003 in the 2dF and 6dF surveys [20] show unresolved Balmer lines ($FWHM \leq 200$ km s^{-1}) and line ratios consistent with a Sy 2 classification (Fig. 6).

The source has been monitored with the SWIFT-XRT since its discovery. The SWIFT observations have been analysed following the procedure outlined in Evans et al. (2009) [21] and show stable soft X-ray emission to within a factor 2 (Fig. 7).

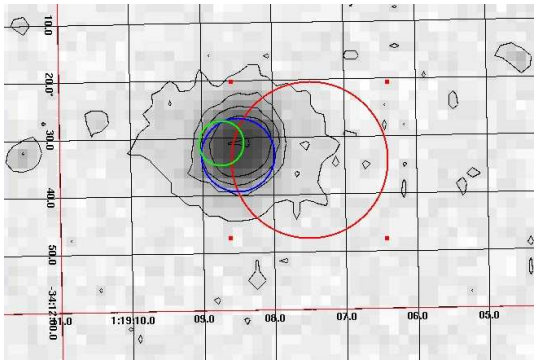

Figure 5: A DSS image and contours of GSN 069: the red circle represents the XMM-Newton slew error circle, blue is for the SWIFT-XRT position and green is the SWIFT position enhanced using UVOT

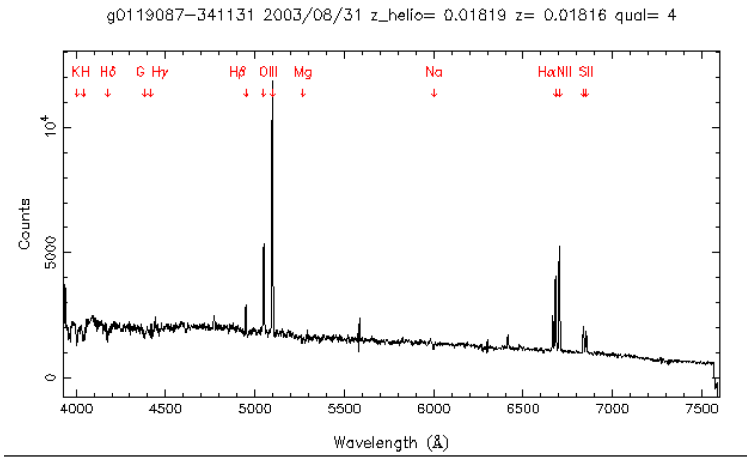

Figure 6: Optical spectrum of GSN 069 from the 6dF survey

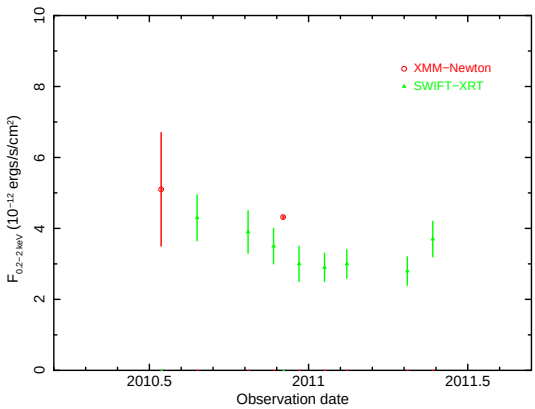

Figure 7: The X-ray light curve of GSN 069

Table 2: GSN 069 observation log

Mission[a]	Date	Count rate[b]	Flux[c]
RASS	1990	< 0.0099	< 0.11
ROSAT-PSPC	1993-07-13T04:38:55	< 0.00177	< 0.019
ROSAT-PSPC	1994-06-29T05:59:51	< 0.00129	< 0.014
XMM slew	2010-07-14T00:48:14	1.49 ± 0.35	5.1 ± 1.6
SWIFT	2010-08-27T06:05:40	0.041 ± 0.005	4.3 ± 0.6
SWIFT	2010-10-27T05:32:30	0.037 ± 0.004	3.9 ± 0.6
SWIFT	2010-11-24T01:19:48	0.033 ± 0.004	3.5 ± 0.5
XMM pointed	2010-12-02T10:44:18	1.03 ± 0.01	4.32 ± 0.04
SWIFT	2010-12-22T15:05:03	0.029 ± 0.004	3.0 ± 0.5
SWIFT	2011-01-19T06:15:29	0.028 ± 0.004	2.9 ± 0.4
SWIFT	2011-02-16T05:33:31	0.029 ± 0.003	3.0 ± 0.4
SWIFT	2011-04-25T05:00:28	0.027 ± 0.003	2.8 ± 0.4
SWIFT	2011-05-23T04:06:01	0.035 ± 0.004	3.7 ± 0.5

[a] XMM-Newton, EPIC-pn camera: slew observation performed in FullFrame mode with the Medium filter; pointed observation performed in FullFrame mode with the Thin filter. SWIFT-XRT in pc mode.
[b] counts s^{-1} in the band 0.2–2 keV.
[c] Unabsorbed flux, $F_{0.2-2\ keV}$, units of 10^{-12} erg s^{-1} cm^{-2}, calculated from a black body model with kT=58 eV and Galactic absorption ($2.48 \times 10^{20} cm^{-2}$)

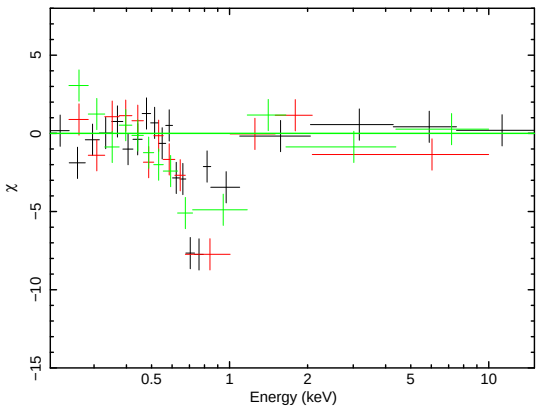

Figure 8: Residuals to a *diskbb* model fit to the XMM-Newton EPIC-pn (black), MOS-1 (red) and MOS-2 (green) data

4.1 X-ray spectral fits

An XMM-Newton TOO, with nominal exposure 10ks, was performed in December 2010, using all of the X-ray detectors and the optical monitor. The data were reduced using XMM-SAS v11.0 ([15]). EPIC source spectra were extracted from a circle of 30 arcsecond radius and background taken from a nearby source-free region. The two RGS cameras were combined into one spectrum. All the camera spectra were grouped so as to contain a minimum of 25 counts per bin and to oversample the instrument resolution by a maximum of 3. Fits to the individual instruments gave consistent results and so all spectra were fit simultaneously, with a constant used to compensate for the small normalisation differences.

An initial fit with a power-law, absorbed by the Galactic column (2.48×10^{20}; LAB Map - [23]) gave a poor fit but showed that the overall spectrum is very soft ($\Gamma = 6.2$). To model the shape better we fit the soft X-rays with a black-body or multi-colour disk model (diskbb in XSPEC) and the weak emission at > 2 keV with a power-law (with Γ fixed to 1.7). The black-body and diskbb models yielded better fits with $\chi^2_r = 1.4, 2.0$ respectively (Tab. 3). To fit the remaining residuals we tried various absorption models. Cold absorption, in the rest frame of the source, is excluded with an upper limit of 9×10^{19}cm^{-2}. Good fits were obtained with a simple edge of energy 650 eV or with an ionized absorber with N_H=4-11$\times 10^{23}$cm^{-2}, $\xi = 100 - 800$ and a covering fraction of 74–100% redshifted by either 0.15 or 0.2 in the rest frame of the source, depending on the continuum model (Fig. 8).

The unabsorbed soft X-ray luminosity is $L_{0.2-2} = 5.3 \pm 0.1 \times 10^{42}$ erg s^{-1} for the best fit model (diskbb with edge). This model greatly underpredicts the flux observed in the OM UVW1, UVM2 and B filters. However, the optical images of the galaxy appear extended in all filters and so the count rates are clearly dominated by emission from the stellar population. We therefore extrapolate the soft X-ray spectral model over optical, UV and EUV frequencies to obtain $L_{bol} = 1.8 \pm 0.1 \times 10^{43}$ erg s^{-1}. The emission above 2 keV is very weak, $1.1 \pm 0.9 \times 10^{-3}$ counts s^{-1} in the EPIC-pn detector, and the conversion of this count rate to an unabsorbed flux is highly model dependent. We find a highest, 90% confidence, upper limit of $L_{2-10} < 8.5 \times 10^{40}$ erg s^{-1}, for the black-body with partial covering model.

A spectral fit of the combined SWIFT-XRT data gives very similar spectral parameters to the XMM-Newton spectrum showing that the soft spectral shape of GSN 069 is long lasting.

A possible explanation for the steep X-ray spectra of GSN 069 is provided by an ionized absorber which allows very soft X-rays to pass while strongly blocking higher energies. This model was used to explain the very steep spectra of WPVS 007 seen during the ROSAT era [24]. To test for this we have attempted to fit the GSN 069 XMM-Newton spectrum with intrinsic power-law emission absorbed by up to three ionized, partial covering, absorbers. No good fit was obtained with a power-law model with $\Gamma < 4$ and therefore we conclude that the very steep soft X-ray spectrum is thermal in origin.

4.2 Discussion

The lack of a cold absorber in the X-ray spectrum of GSN 069 is difficult to reconcile with the classical interpretation of a Sy II where the broad lines are removed by absorption. From the 6dF optical spectrum we find a ratio of [OIII]5007 / $H_\beta \sim 11$ which is symptomatic of a missing

Table 3: GSN 069 spectral fits to an XMM-Newton TOO

Low-energy model				Intrinsic absorption						χ^2/dof
Plaw	Bbody	Diskbb		Edge[a]		zxipcf[b]				
Γ	kT (ev)	kT (eV)	Norm	E (eV)	Tau	N_H	ξ	cf(%)	z	
6.2	-	-	-	-	-	-	-	-	-	2015/107
-	$56.3^{+0.7}_{-0.3}$	-	-	-	-	-	-	-	-	152/107
-	$58.2^{+0.7}_{-0.5}$	-	-	651^{+22}_{-13}	$0.80^{+0.27}_{-0.19}$	-	-	-	-	116/105
-	$62.2^{+0.7}_{-0.6}$	-	-	-	-	98^{+10}_{-18}	$2.7^{+0.1}_{-0.7}$	82^{+4}_{-8}	$0.167^{+0.005}_{-0.008}$	114/103
-	-	67.1	43695	-	-	-	-	-	-	215/107
-	-	$71.7^{+0.9}_{-0.9}$	28184^{+370}_{-470}	650^{+16}_{-11}	$1.44^{+0.29}_{-0.24}$	-	-	-	-	112/105
-	-	$77.4^{+1.1}_{-2.0}$	21105^{+340}_{-460}	-	-	54^{+9}_{-10}	$2.8^{+0.1}_{-0.6}$	92^{+8}_{-8}	$0.225^{+0.007}_{-0.007}$	116/103

All fits included absorption by the Galactic column ($N_H = 2.48 \times 10^{20}$cm^{-2}) and a power-law with slope fixed at $\Gamma = 1.7$ to model the very weak emission beyond 2 keV. Errors are 90% confidence. [a] The *edge* model in *XSPEC*. [b] A partially ionized, partial covering model (*zxipcf* in *XSPEC*) with parameters, N_H in units of 10^{22}cm^{-2}, log of the ionization parameter, covering fraction and redshift.

BLR rather than absorption in Sy II [31]. From this we conclude that the BLR is absent rather than obscured in this case. In other words, GSN 069 appears to be another example of an AGN classified as a Sy II galaxy but with little or no intrinsic absorption in the X-rays and with optical line ratios inconsistent with heavy extinction. The X-ray spectrum could be reconciled with a Sy II classification if the AGN was Compton-thick in the X-rays (although the optical line ratios do not support this idea). However the soft X-ray variability on both short (doubling time of 800s in the XMM-Newton observation) and long (see Table 2) timescales rules out this hypothesis, making GSN 069 a "true Sy II" candidate, i.e. a candidate AGN with no BLR.

In the paradigm where the BLR is created from outflows of material from the disk, the outflow may not be sustainable and hence the BLR may be absent if $L_{bol} < 10^{42}$ erg s^{-1} [26] or if the accretion rate is below a critical value $\dot{m} < 0.01$ [25].

The black hole mass, M_{BH}, can be estimated from the normalisation of the *diskbb* model if the emission is thermal, as it seems to be. Following Yuan et al. 2010 [30], and taking the disk inclination as i=40° for simplicity, we derive the black hole mass as $M_{BH} = 1.7 \times 10^5$ M$_\odot$ for a non-rotating black hole and $M_{BH} = 8.4 \times 10^5$ M$_\odot$ for a maximally spinning Kerr black hole. The accretion rate may be derived from the z-corrected temperature, to be $\dot{m} = 0.017 - 0.38$ depending on the black hole spin. An independent estimate of M_{BH} may be found from its relationship with the bulge K band luminosity [28]. The 2MASS extended catalogue gives m$_K$=12.75, for the whole galaxy, which implies $M_{BH} < 2.5 \times 10^6$ M$_\odot$. The low mass of the black hole is also supported, to some extent, by fast variability (doubling time of 800s) seen in the XMM-Newton light curve.

From the relationship between M_{BH}, $\dot{m}$ and the FWHM of the BLR lines [6] we would expect to be seeing broad lines with FWHM=560-1800 km s^{-1} in the optical spectrum.

The luminosity of the [OIII]5007 line in the 6dF spectrum is 1.1×10^{40} erg s^{-1} which implies

a historical $L_{bol} \sim 10^{42}$ erg s^{-1} using a bolometric correction factor of 88–142 [29]; an order of magnitude below the current value. If radiating at an efficiency $\eta = 0.1$, the historical accretion rate will have been $\dot{m} = 0.009 - 0.047$. In the past then, the source has been accreting and radiating close to the critical values necessary to produce outflows and plausibly has been too weak to produce the BLR. With the current AGN parameters an outflow should be sustainable, in which case we can estimate the time necessary to form the BLR as $t = v/d$, where v is the velocity of expanding material and d is the distance of the BLR which will be ~ 10 days for $L_{bol} = 10^{43}$ erg s^{-1} [32]. Hence for outflow velocities of 1000-6000 km s^{-1} (e.g. [27]) BLR material will start to build up after 2-12 months. A regular monitoring of the optical spectrum of GSN 069 may be able to detect this process.

The apparently redshifted, strong edge observed at ~ 650 eV may be produced by a failed disk outflow or from an inflowing accretion disk overlapping our line of sight.

In summary, the soft emission from this SY II appears to be thermal in origin and its variability appears to be intrinsic to the central engine and not related to changes in line-of-sight absorption. This mechanism may also be the cause of the strong variability seen in the other Sy II galaxies, three of which have $L_X < 10^{43}$ erg s^{-1} in their high state.

References

[1] Vaughan, S., Uttley, P., Pounds, K.A., Nandra, K., Strohmayer, T.E.: *The rapid X-ray variability of NGC 4051*, MNRAS, 413, 2489 (2011).

[2] Markowitz, A., Papadakis, I., Arevalo, P., Turner, T.J., Miller, L., Reeves, J.N,: *The Energy-dependent X-Ray Timing Characteristics of the Narrow-Line Seyfert 1 Mrk 766*, ApJ, 656, 116, (2007).

[3] McHardy, I. & Czerny, B.: *Fractal X-ray time variability and spectral invariance of the Seyfert galaxy NGC5506*, Nature 325, 696 (1987).

[4] McHardy, I. M., Papadakis, I. E., Uttley, P., Mason, K. O., Page, M. J.: *Combined long and short timescale X-ray variability of NGC 4051 with RXTE and XMM-Newton*, In: Nuclear Physics B Proceedings Supplements, Volume 132, p. 122 (2004).

[5] Edelson, R. & Nandra, K., *A Cutoff in the X-Ray Fluctuation Power Density Spectrum of the Seyfert 1 Galaxy NGC 3516*, ApJ, 514, 682 (1999).

[6] McHardy, I., Koerding, E.; Knigge, C.; Uttley, P.; Fender, R. P: *Active galactic nuclei as scaled-up Galactic black holes*, Nature, 444, 730 (2006).

[7] Risaliti, G.; Elvis, M.; Fabbiano, G.; Baldi, A.; Zezas, A. *Rapid Compton-thick/Compton-thin Transitions in the Seyfert 2 Galaxy NGC 1365*, ApJ, 623, L93 (2005).

[8] Risaliti, G.; Miniutti, G.; Elvis, M.; Fabbiano, G.; Salvati, M.; Baldi, A.; Braito, V.; Bianchi, S.; Matt, G.; Reeves, J. *Variable Partial Covering and A Relativistic Iron Line in NGC 1365*, ApJ, 696, 160 (2009).

[9] Giommi, P.; Barr, P.; Pollock, A. M. T.; Garilli, B.; Maccagni, D.: *A study of BL Lacertae-type objects with Exosat. I - Flux correlations, luminosity variability, and spectral variability*, ApJ, 356, 432 (1990).

[10] Voges, W., Aschenbach, B., Boller, T.,Braeuninger, H., Burkert, W., Dennerl, K., Englhauser, J., Gruber, R., Haberl, F., *et al.*: *The ROSAT all-sky survey bright source catalogue*, A&A, 349, 389. (1999).

[11] Saxton, R., Read, A M., Esquej, P., Freyberg, M. J., Altieri, B., Bermejo, D. *The first XMM-Newton slew survey catalogue: XMMSL1*, A&A, 480, 611 (2008).

[12] Zimmerman, H. U., Becker, W., Belloni, T., *et al. EXSAS User's guide*. In: *MPE Rep, 257* (1994).

[13] Saxton, R. & Diaz-Toledo Gimeno, C.: *ULS: An upper limit server for X-ray and Gamma-ray astronomy*. In: ASP Conf. Ser., Vol. 442, ADASS XX ed. I. N. Evans, Accomazzi, A., Mink, D. J. & Rots, A. H., 567 (2011).

[14] Mittaz, J. P. D., Carrera, F. J., Romero-Colmenero, E., Mason, K. O., Hasinger, G., McMahon, R., Andernach, H., Bower, R., Burgos-Martin, J., GonzÃąlez-Serrano, J. I., Wonnacott, D: *X-ray spectra of the RIXOS source sample*, MNRAS, 308, 233 (1999).

[15] Gabriel, C. *et al.* : , In ASP Conf. Ser., Vol. 314, ADASS Xiii ed. Oschenbein, F., Allen, M. & Egret, D. 759 (2003).

[16] Almaini, O, *et al.*: *X-ray variability in a deep, flux-limited sample of QSOs*, MNRAS, 315, 325 (2000).

[17] Mateos, S., Barcons, X., Carrera, F. J., Page, M. J., Ceballos, M. T., Hasinger, G., Fabian, A. C.: *XMM-Newton observations of the Lockman Hole. V. Time variability of the brightest AGN*, A&A, 473, 105 (2007).

[18] MacLeod, C. L. *et al.*: *Modeling the Time Variability of SDSS Stripe 82 Quasars as a Damped Random Walk*, ApJ, 721, 1014 (2010).

[19] Clavel, J., Nandra, K., Makino, F., Pounds, K. A., Reichert, G. A., Urry, C. M., Wamsteker, W., Peracaula-Bosch, M., Stewart, G. C.: *Correlated hard X-ray and ultraviolet variability in NGC 5548*, ApJ, 393, 113 (1992).

[20] Jones, D. H., Saunders, W., Colless, M., Read, M. A., Parker, Q. A.; Watson, F. G.; Campbell, Lachlan A.; Burkey, D., Mauch, T., Moore, L., *et al.*: *The 6dF Galaxy Survey: samples, observational techniques and the first data release*, MNRAS, 355, 747 (2004).

[21] Evans P.A., *et al.*: *Methods and results of an automatic analysis of a complete sample of Swift-XRT observations of GRBs*, MNRAS, 397, 1177 (2009).

[22] Veron-Cetty, M. P. & Veron, P.: *Veron Catalog of Quasars & AGN, 12th edition*, A&A, 455, 776 (2006).

[23] Kalberla, P. M. W.; Burton, W. B.; Hartmann, Dap; Arnal, E. M.; Bajaja, E.; Morras, R.; PÃűppel, W. G. L.: *The Leiden/Argentine/Bonn (LAB) Survey of Galactic HI. Final data release of the combined LDS and IAR surveys with improved stray-radiation corrections*, A&A, 440, 775 (2005).

[24] Grupe, D., Leighly, K. M., Komossa, S.: *First Detection of Hard X-Ray Photons in the Soft X-Ray Transient Narrow-Line Seyfert 1 Galaxy WPVS 007: The X-Ray Photon Distribution Observed by Swift*, AJ, 136, 234 (2008).

[25] Nicastro, F.: *Broad Emission Line Regions in Active Galactic Nuclei: The Link with the Accretion Power*, ApJ, 530, L65 (2000).

[26] Elitzur, M. & Shlosman, I.: *The AGN-obscuring Torus: The End of the "Doughnut" Paradigm?*, ApJ, 648, L101 (2006).

[27] Leighly, K., Hamann, Fred; Casebeer, Darrin A.; Grupe, Dirk.: *Emergence of a Broad Absorption Line Outflow in the Narrow-line Seyfert 1 Galaxy WPVS 007*, ApJ, 701, 176 (2009).

[28] Marconi, A., Hunt, L. K. *The Relation between Black Hole Mass, Bulge Mass, and Near-Infrared Luminosity*, ApJ, 589, L21 (2003).

[29] Lamastra, A., Bianchi, S., Matt, G., Perola, G. C., Barcons, X., Carrera, F. J.: *The bolometric luminosity of type 2 AGN from extinction-corrected [OIII]. No evidence of Eddington-limited sources*, A&A, 504, 73 (2009).

[30] Yuan, W., Liu, B. F., Zhou, H. & Wang, T. G.: *X-ray observational signature of a black hole accretion disk in an active galactic nucleus RX J1633+4718*, ApJ, 723, 508 (2010).

[31] Hawkins, M. R. S.: *Naked active galactic nuclei*, A&A, 424, 519 (2004).

[32] Denney, K. D., Peterson, B. M., Pogge, R. W., Adair, A., Atlee, D. W., Au-Yong, K., Bentz, M. C., Bird, J. C., Brokofsky, D. J., Chisholm, E.: *et al.*: *Reverberation Mapping Measurements of Black Hole Masses in Six Local Seyfert Galaxies*, ApJ, 721, 715 (2010).

5. Acknowledgements

The XMM-Newton project is an ESA science mission with instruments and contributions directly funded by ESA member states and the USA (NASA). This work made use of data supplied by the UK Swift Science Data Centre at the University of Leicester. We thank Jane Turner and Lance Miller for useful discussions about ionized absorber models.